

Fig. 1. Voltammograms of enoximone in pH 1.5 media. Background and single scan after three additions of enoximone.

It is evident that the entire oxidation wave is shifted at least 150 mV negative of those found at the unconditioned CPE.

This phenomenon is not fully understood and, while uncommon, is not unknown. Blaedel and Jenkins reported a

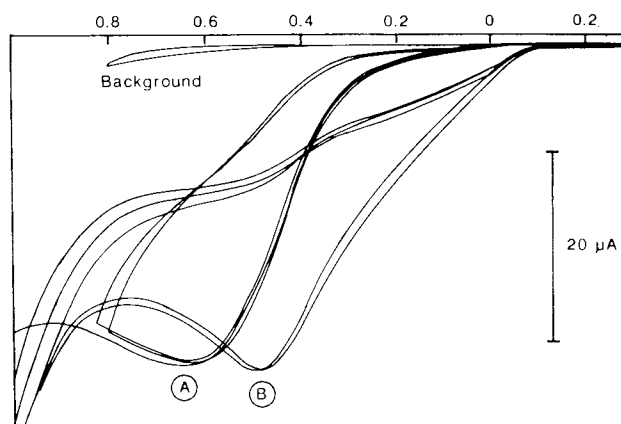


Fig. 2. Voltammograms of enoximone in pH 12.5 media. (A) At resurfaced, nonconditioned CPE. (B) After CPE modified by scanning to +1.2 V.

negative potential shift for the oxidation wave of NADH at a glassy carbon electrode following pretreatment of the electrode (2). Their pretreatment procedure consisted of 15 constant potential steps (+1.5, -1.5V). They speculated that oxides could be formed at the electrode surface and facilitate electron transfer through the electrode boundary layer. Our further evaluation of the oxidation wave shift may be seen in the peak potential data in Table I. The effect is pronounced only in basic media where enoximone is ionized ($pK_a = 10.3$). The resulting implication is that ionized enoximone

Table I. Peak Potentials and Peak Current Constants for Enoximone at a Carbon Paste Electrode

Buffer	pH	E_p (V) ^a			$E_p - E_{p/2}$ (V) ^b	Current constant ($\mu A/mM$) ^a				
H ₂ SO ₄	1.5	1.01	1.02	1.03	0.077	117	115	115		
		1.05*	1.08*	1.08*		1.05	132	135	133	130
		1.01	1.02	1.02		1.03	130	130	124	
Glycine	3.8	1.05*	1.06*	1.07*	0.079	120	127	129	138	
		1.02	1.03	1.04		1.04	111	112	113	
Citrate	4.0	1.07*	1.05*	1.08*	0.080	104	114	113	116	
		1.01	1.02	1.03		1.06	108	107	108	
Citrate	5.1	1.07*	1.07*	1.10*	0.100	112	118	110	106	
		0.99	1.00	1.00		1.08*	103	102	101	108
Acetate	6.2	1.09*	1.07*	1.09*	0.095	125	108	114	109	
		1.02	1.03	1.06		1.07	96	95	95	
Citrate	7.0	1.01	1.02	1.03	0.148	97	97	97	99	
		0.99	1.00	1.02		1.07*	96	96	95	
Tris	7.0	1.03	1.03	1.04	0.160	89	91	92		
		1.03	1.04	1.05		1.07	87	90	92	
Tris	8.6	1.00	1.00	1.02	0.280	101	97	88	90	
		0.94	0.94	0.94		1.06*	69	69	68	76
Glycine	10.0	0.80	0.82	0.83	0.340	68	66	65	70	
		0.94*	0.94*	0.94*		—	68	66	65	70
LiOH	12.5	0.43	0.45	0.47	0.220	58	60	56	62	
		0.65*	0.50	0.48		0.67*	62	63	62	

^a Values with superscript asterisks were obtained at a freshly resurfaced CPE. Values were obtained in sequence, reading from left (lowest concentration) to right in the peak potential (E_p) and current constant columns. Data on each line are from separate experiments usually acquired several months apart.

^b Peak potential - potential where current is one-half that at the peak. Measured at the highest concentration voltammogram obtained at a freshly resurfaced CPE.

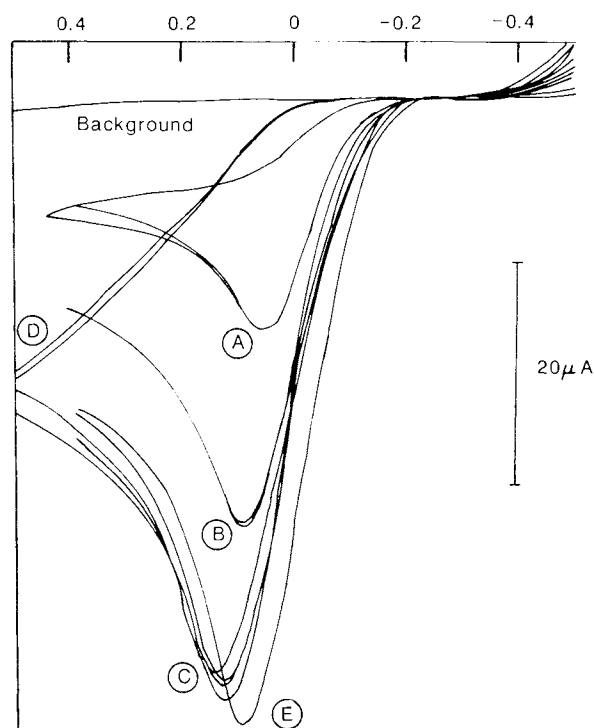


Fig. 3. Voltammograms of MIO in pH 12.5 media. (A–C) After sequential additions of compound (replicate scans) at a conditioned CPE. (D) On same solution as C but at a freshly resurfaced CPE. (E) On same solution as D, after conditioning the CPE at +1.2 V for less than 30 sec.

may be a useful probe in other studies of electrode surface modification.

Data illustrating analytical capability and pH effects are shown in Table I. With a given electrode, good reproducibility and response linearity are observed. Buffer effects are not very significant but two pH effects are noted. First, peak current responses decrease essentially linearly with pH until the response at high pH is about half that at low pH. Second, effects of deprotonation of the dihydroimidazolone function are noted as the peak oxidation potential decreases at -137 mV/pH above an apparent pH of 8.5.

Assignment of electrochemical activity to molecular

functionality was simplified by evaluation of 4-(methylthio)benzoic acid (MTBA) and 4-methyl-1,3-dihydroimidazol-2-one (MIO). The MTBA molecule is not oxidized at the CPE below +1.3 V. However, MIO is easily oxidized (+0.9 V acidic, *ca.* +0.1 V basic) to account for the observed electrochemistry of enoximone. Current constants are *ca.* $120 \mu\text{A}/\text{mM}$ in acidic media and *ca.* $150 \mu\text{A}/\text{mM}$ in strongly basic media—*i.e.*, similar to enoximone at low pH but *ca.* twice the response of enoximone at high pH. At least part of this difference is probably due to a higher $\text{p}K_a$ for MIO than for enoximone. Similar, but more pronounced, effects of fresh and preconditioned CPE surfaces are also observed (Fig. 3). The MIO molecule is smaller and much more water soluble than enoximone, so it would be expected to have less physical affinity for the CPE. The generation of new functionalities at the conditioned CPE would be expected to make this a relatively less hostile environment as well as facilitate electron transfer.

Coulometric data indicate that enoximone and MIO undergo a two-electron oxidation (Table II). In acidic media, enoximone oxidation results in two products, which have similar chromophores ($\lambda_{\text{max}} = 320$ nm) as enoximone and relative retention times (RRT) of 0.74 and 0.85, respectively, when evaluated by HPLC. Also, MTBA is observed ($\lambda_{\text{max}} = 280$ nm, RRT = 1.6). In basic media, enoximone oxidation consumes between two and three electrons. MTBA is observed as a product, and when observed, it is produced stoichiometrically from the enoximone oxidized. Otherwise, another product of enoximone's oxidation occurs at 0.74 RRT, but its absorption maximum is 280 nm, rather than 320 nm as observed for a product at this RRT from electrolysis in acid. From these data, we conclude that the initial oxidation is a two-electron transfer, resulting in an unstable imidazolone function which then undergoes hydrolytic ring opening to two products. These products may then undergo further hydrolysis/electrolysis to account for the overall results, including the appearance of MTBA. Better understanding of the reaction mechanism(s) would require conclusive identification of the observed products, studies of their electrochemical characteristics, and evaluation of their chemical stabilities.

Piroximone behaves similarly to enoximone at the CPE (Table III). However, peak potentials are at least 100 mV

Table II. Coulometry Data for Enoximone and MIO at a Carbon Paste Electrode

Sample	Buffer	pH	CPE ^a	E (V)	Time (min)	% oxidized ^b	n	MTBA found
MIO	LiOH	12.5	R	+0.7	60	76.5	2.06	—
	LiOH	12.5	M	+0.3	60	83.5	2.06	—
Enoximone	H ₂ SO ₄	1.5	R	+1.1	86	56.3	2.07	Yes
	LiOH	12.5	R	+0.8	90	52.5	2.38	Yes
	LiOH	12.5	R	+0.7	120	43.3	2.10	No
	LiOH ^c	12.2	R	+0.7	60	21.8	2.12	No
	LiOH	12.5	M	+0.8	120	95.5	2.74	Yes
	LiOH	12.5	M	+0.3	90	41.6	2.04	No
	LiOH	12.5	M	+0.3	60	60.8	2.15	Yes

^a R, electrode resurfaced prior to coulometry. M, electrode modified at +1.2 or +1.4 V prior to coulometry.

^b As determined by HPLC analysis.

^c Electrolyte was 100% 0.05 M LiOH.

Table III. Peak Potential and Peak Current Constants for Piroximone at a Carbon Paste Electrode

Buffer	pH	E_p (V) ^a			$E_p - E_{p/2}$ (V)	Current constant ($\mu A/mM$) ^a		
		1.12	1.14	1.15		148	142	136
H ₂ SO ₄	1.60	1.12	1.14	1.15	0.07	148	142	136
		1.16	1.17	1.18	0.10	131	129	127
Glycine	3.39	1.11	1.14	1.16	0.09	148	140	135
Citrate	3.55	1.10	1.12	1.13	0.09	126	120	115
Citrate	4.54	1.09	1.11	1.14	0.09	129	124	119
Acetate	5.30	1.09	1.12	1.15	0.12	134	128	125
		1.11	1.12	1.13	0.09	128	121	120
Citrate	5.51	1.09	1.11	1.13	0.10	126	122	117
Acetate	6.33	1.11	1.14	1.15	0.11	135	133	132
Citrate	6.46	1.09	1.11	1.11	0.09	125	118	121
Tris	7.05	1.09	1.11	1.13	0.10	131	128	125
Tris	7.89	1.10	1.16	1.19	0.15	101	89	83
Tris	8.85	1.06	1.10	1.13	0.16	92	89	89
Glycine	8.87	1.05	1.07	1.09	0.16	108	103	99
Glycine	9.92	0.95	0.97	0.98	0.24	94	89	84
		0.51	0.51	0.51	0.25	60	57	57
LiOH	12.38	0.57	0.57	0.57	0.17	65	68	67
		0.51	0.51	0.51	0.25	60	57	57

^a Data are given for the averages of two scans taken after each of three sample additions to the electrolyte. Read peak potential (E_p) and current constant columns from left to right.

^b The CPE was resurfaced prior to this scan.

more positive and current constants are somewhat larger. The shift in oxidation potential parallels the greater electron withdrawing capacity of the 4-pyridoyl function compared to the 4-(methylthio)benzoyl function.

Table IV. Coulometry Data for Piroximone at a Carbon Paste Electrode

Buffer	pH	E (V)	Time (min)	% oxidized ^a	n
H ₂ SO ₄	1.60	1.15	90	40.9	2.0
H ₂ SO ₄	1.60	1.15	92.5	33.8	2.4
H ₂ SO ₄	1.60	1.09	150	15.8	2.1
Acetate	5.30	1.15	90	68.1	2.9
Acetate	5.30	1.15	90	66.9	3.0
Acetate	5.30	1.00	105	18.5	2.8

^a As determined by HPLC analysis.

Current constants of piroximone are higher at lower concentrations, which suggests absorption of piroximone at the CPE. Since this effect is not obvious with enoximone, a tentative causal relationship was assigned to the ethyl-imidazolone function of piroximone. However, when the methyl-imidazolone analogue of piroximone was examined, similar behavior was observed at pH 1.6 and pH 12.38. Lower current constants and better linearity were found at pH 5.3, however, so these limited data are supportive of the hypothesis only at pH 5.3.

Coulometric data from pH 1.6 and pH 5.3 media show *ca.* 2 electrons/molecule, and *ca.* 3 electrons/molecule, respectively (Table IV). At lower pH, an oxidation product containing the 322-nm chromophore of piroximone was detected by HPLC (RRT 0.6). This product was not observed from the higher-pH coulometric experiments, but an increase in absorbance was noted in the HPLC solvent front. Since isonicotinic acid elutes in the solvent front and since

Table V. Reductive Peak Potential and Peak Current Constants for Piroximone at a Mercury Electrode

Buffer	pH	Voltammetry			Differential pulse polarography ^a			
		E_p^a (V)	$E_p - E_{p/2}^a$ (V)	Current constant ($\mu A/mM$) ^b	E_p (V)	Apparent current constant ($\mu A/mM$)		
H ₂ SO ₄	1.60	-0.47	0.02	11.5	11.7	11.7	-0.45	70.1
		-0.48	0.02	12.5	12.4	12.4	-0.46	75.1
		-0.47	0.03	11.8	11.8	11.8	-0.45	72.4
Glycine	3.39	-0.47	0.03	11.8	11.8	11.8	-0.45	72.4
Citrate	3.55	-0.56	0.03	12.4	12.6	12.7	-0.53	77.3
Citrate	4.54	-0.63	0.03	11.2	11.4	11.5	-0.60	69.7
Acetate	5.30	-0.68	0.04	11.5	11.6	12.0	-0.60	67.4
		-0.69	0.03	11.4	11.5	11.5	-0.65	67.8
		-0.68	0.03	11.2	11.4	11.4	-0.66	66.0
		-0.69	0.03	11.3	11.3	11.6	-0.67	67.1
		-0.70	0.04	10.3	10.4	10.5	-0.67	55.5
Acetate	6.33	-0.77	0.05	9.3	9.3	9.4	-0.73	48.7
Citrate	6.46	-0.79	0.03	8.3	8.2	8.2	-0.74	33.9
Tris	7.05	-0.81	0.04	9.7	9.9	9.9	-0.78	63.3
Tris	7.89	-0.86	0.04	9.0	9.3	9.9	-0.82	70.7
Tris	8.85	-0.95	0.07	8.0	7.6	8.0	-0.88	49.1
Glycine	8.87	-0.99	0.09	6.9	6.7	7.2	-0.92	19.6
Glycine	9.92	-1.15	0.11	7.9	7.5	7.5	-1.11	24.3
LiOH	12.38	-1.32	0.07	7.5	8.1	8.4	-1.28	37.0
		-1.32	0.05	8.4	8.5	8.6	-1.27	36.4

^a Measurements performed on final solution used in voltammetry.

^b Peak current responses measured after each of three sequential additions of sample.

4-(methylthio)benzoic acid was observed in the enoximone study, preliminary speculation focuses on isonicotinic acid as one of the products. It is observed also as a product of degradation of piroximone in basic media (3).

Piroximone is reduced at the HMDE with no evidence of oxidation peaks when evaluated by cyclic voltammetry (0 to -1 V at 100 mV/sec). Voltammetric and differential pulse polarographic data are shown in Table V. Excellent assay sensitivity and linearity are obtained. Even though electron transfer is irreversible, electron transfer kinetics are rapid, and sharp voltammetric responses occur. Between pH 3.55 and pH 8.85 peak potentials become more negative at -0.072 V/pH. Discontinuities in the peak potential-versus-pH plot occur in acidic media around pH 3 and in basic media around pH 9, reflecting effective pK_a values of 3.3 and 9.6 for the protonated pyridyl and the imidazolone functions (4).

Enoximone is not electrochemically reducible in these media. Isonicotinic acid is reducible at -0.84 V in pH 1.6 media and at -1.10 V in pH 5.3 media. Additionally, the 3-pyridyl analogue of piroximone is reducible at -0.75 and -0.89 V in pH 1.6 and pH 5.3 media, respectively. Extended conjugation in piroximone increases its ease of reduction relative to the congeners. The conjugation effect is also noted as the UV absorption maximum of 265 nm for isonicotinic acid is shifted to 322 nm for piroximone. Similar current constants are obtained for the analogue and isonicotinic acid as for piroximone. Inferentially, then, the reductive behavior of piroximone is attributable to its pyridoyl function.

Table VI. Determination of Piroximone at Low Levels By Differential Pulse Polarography

Concentration $\times 10^7$ M	E_p (V)	Peak current (μA) ^a	Apparent current constant ($\mu A/mM$)
0.72	-0.44	0.0122^b	169
1.61	-0.46	0.0281	175
2.51	-0.46	0.0434	173

^a Obtained in H_2SO_4 electrolyte at a scan rate of 2 mV/sec and a pulse amplitude of 50 mV.

^b Value is ca. $6\times$ baseline noise.

Quantitation of enoximone and piroximone in HPLC effluent is easily, sensitively, and reproducibly achieved with an amperometric detector. Repetitive injections of 7.0 and 1.77 ng of enoximone resulted in 2.36 ± 0.05 and 0.58 ± 0.02 nA, respectively, for four injections of each solution. These results were obtained with enoximone eluting at 11.4 ml ($k' = 2.8$), with an applied potential of $+1.0$ V. An optimized chromatographic system, particularly one employing more efficient column packings, would improve detection sensitivity considerably. In those instances where specificity is an issue, it may be possible to use mobile phases with pH greater than 7 or postcolumn reactors to pH the column effluent above 7 to permit quantitation of these cardiotonics at much lower potential. Comparisons of enoximone standards show that the amperometric detector is about 10-fold more sensitive than the UV detector at 320 nm. However, the UV detector at 320 nm is insensitive to many more common sample matrix interferences than the amperometric detector at $+1.0$ V. Choices between these detectors often is determined by the overall sensitivity requirement of the experiment and the amount of sample preparation necessary to maintain specificity at low concentrations.

Differential pulse polarography was evaluated here because of its characteristic sensitivity. In solution studies where turbidity or opaqueness interferes with UV detectors, determination of low levels of piroximone may be undertaken with DPP. Examples of sensitivity and linearity are shown in Table VI (slope = $0.174 \mu A/mM$, where detector baseline noise is about $0.02 \mu A$).

REFERENCES

1. K. T. Weber, S. K. Gill, J. S. Janicki, C. S. Maskin, and M. C. Jain. Newer positive inotropic agents in the treatment of chronic cardiac failure. *Drugs* 33:503-519 (1987).
2. W. J. Blaedel and R. A. Jenkins. Study of the electrochemical oxidation of reduced nicotinamide adenine dinucleotide. *Anal. Chem.* 47:1337-1342 (1975).
3. T.-M. Chen, J. E. Coutant, A. D. Sill, and R. R. Fike. Thermospray high-performance liquid chromatographic-mass spectrometric analysis of the degradation products of piroximone. *J. Chromatogr.* 396:382-388 (1987).
4. W. H. Streng and H. G. H. Tan. General treatment of pH solubility profiles of weak acids and bases. II. Evaluation of thermodynamic parameters from the temperature dependence of solubility profiles applied to a zwitterionic compound. *Int. J. Pharm.* 25:135-145 (1985).